Steel and Composite Structures, Vol. 7, No. 6 (2007) 469-486
DOI: http://dx.doi.org/10.12989/scs.2007.7.6.469

Ultimate load behaviour of tapered steel plate girders

N. E. Shanmugam†

Department of Civil and Structural Engineering, Universiti Kebangsaan Malaysia, Bangi, Malaysia

Hu Min‡

Department of Civil Engineering, National University of Singapore, Singapore

(Received May 16, 2007, Accepted November 30, 2007)

Abstract. The paper is concerned with the behavior of tapered steel plate girders, primarily subjected to shear loading; experimental as well as finite element results obtained from the studies are presented in this paper. In the experimental study, 11 large-scale girders, one of uniform section and 10 tapered, were tested to failure and all girders were analysed by finite element method. The results are compared and the accuracy of the finite element modeling established. A parametric study was carried out with thickness of web, loading direction and taper angle as parameters. An analytical model, based on Cardiff model for girders of uniform cross-section, is also proposed in the paper.

Keywords: plate girder; taper angle; experiment; finite element modelling; ultimate load behaviour; tension field action.

1. Introduction

It is often necessary to introduce openings in the web of plate girders in order to provide space for services, resulting in high cost of fabrication and reduction in load-carrying capacity. An alternative method may be to use plate girders with varying web depth in which the reduced depth near supports provides the required space for services. Engineers are reluctant to use tapered plate girders in the construction of large-span structural element because of complexities associated with the taper angle. The tapered web alters the stress distribution within the member and will, in most cases, influence the collapse behavior. Even though extensive studies have been made on plate girders of uniform section (Calladine 1973, Porter *et al*. 1975, Evans *et al*. 1978, Roberts and Rockey 1979) information available on tapered plate girders is limited.

Rockey and Skaloud (1971, 1972) showed that for plate girders having proportions similar to those employed in civil engineering construction, the ultimate load carrying capacity is influenced by the flexural rigidity of the flanges. It was shown that the collapse mode of plate girders involved development of plastic hinges in the tension and compression flanges. They conducted ultimate load tests on three series of plate girder models, in each of which only the size of the flanges, and therefore their flexural rigidity, was varied. A more generally applicable mechanism was proposed by Porter *et al*. (1975,

†Professor, Corresponding Author, E-mail: shan@vlsi.eng.ukm.my
‡Graduate Student

1978), and after exhaustive comparisons with test data obtained from various sources the accuracy of these methods have been established. It is assumed in this method that failure will occur when a certain region of the web yields as a result of the combined effect of the inclined tensile membrane stress field and the web buckling stress when four plastic hinges form in the flanges. Further studies to investigate the effects of pure bending, combined action of shear and bending, edge or patch loading on the behaviour of plate girders have been carried out by other researchers (Owen *et al*. 1970, Rockey, 1968, Calladin, 1973, Roberts *et al*. 1979, 1981, 1983 and 2001, Graciano *et al*. 2002 and 2003). More recent works on plate girders have addressed issues such as composite action in plate girders (Baskar *et al*. 2002 and 2003, Shanmugam *et al*. 2003 and 2006, Ryu *et al*. 2005, Shanmugam), plate girders curved in plan (Shanmugam *et al*. 2003, Jung and White 2006), web openings in horizontally curved plate girders (Lian and Shanmugam 2003 and 2004), plate girder bridge strengthened with external prestressing tendons (Park *et al*. 2005) and vibration based damage monitoring under uncertain temperature conditions for plate girder bridges (Kim *et al*. 2007).

In a web panel bound by two flanges and two vertical stiffeners shear is resisted by web plate up to the elastic load. Any further increase of load does not cause a rapid collapse of the girder but results in the formation of buckles in a waveform parallel to the tensile direction. Development of membrane tension in the web is denoted as tension field action and enables the web to sustain loads well in excess of the elastic critical load. A consequence of the membrane tension in the web is the inward pulling of the flanges, under increasing loads. Eventually, plastic hinges are formed in the flanges leading to collapse of the girder. The collapse of a plate girder could, therefore, be assumed to consist of three contributing factors viz. (i) elastic critical load, (ii) resistance by tension field and (iii) contribution by flanges. Porter *et al*. (1975, 1978) proposed an equilibrium solution for evaluating the ultimate shear (V_s) of a plate girder with slender webs using the above concepts.

The elastic and inelastic behavior of plate girders having uniform cross-section along the span is well understood; a number of theoretical as well as experimental investigations on the ultimate load behavior have been reported and design methods proposed. According to engineering practice, tapered girders will be a good alternative to provide space for services near the supports, without affecting the ultimate load. However, there is no sufficient information available in the literature to understand the ultimate load behaviour of such girders. Only a limited number of published work could be traced on steel girders (Davis and Mandal 1979) and on aluminum girders (Sharp *et al*. 1971, Roberts and Newark 1996). Therefore, an experimental investigation of tapered plate girders with different taper angles will be helpful to understand the behavior and load-carrying capacity of these girders.

In this paper, an experimental study on steel tapered plate girders carried out to study the ultimate load behaviour is reported. The experimental work deals with the elastic and ultimate load behavior of the girders under a point load applied at the mid span. Eleven full-scale girders, one of uniform cross-section and the rest with tapered webs, were tested to failure. The results are compared with finite element models using the computer package ABAQUS (Hibbit *et al*. 1994). An analytical method based on the Cardiff Model (Porter *et al*. 1975, Evans *et al*. 1978) with due consideration for the taper angle is also presented in the paper.

2. Experimental program

Two series of tests were carried out on plate girders fabricated by welding steel plates. One of the flanges was kept horizontal whilst the second was inclined following the depth of the web plate. In one

series (A series), girders were tested with the horizontal flange in tension and, in the other (B series) the horizontal flange remained in compression. In each of the two series, five girders with different taper angles and different web thickness were considered. The test specimens were designed such that they represented plate girders that occur in practice. Typical dimensions in a tapered plate girder are illustrated in Fig 1. Measured dimensions of all specimens are summarized in Table 1.

2.1 Fabrication of the test specimens

All steel plates used for the specimens are hot-rolled of Grade 43A, and complied with the specifications of BS 4360. Web plates of the test specimens were cut from steel sheets of approximately 2.0 mm, 3.0 mm and 4.0 mm. The web depth was varied along the span with larger depth at the mid-span and smaller one at the support. The depth at mid-span of all the girders was kept as 800 mm and at the support it was varied as shown in Table 1 so as to get the required taper angle. All cutting operations were made either by shearing or by sawing with sufficient care taken to minimise or eliminate distortions and fluctuations in material properties. The various components were first assembled by means of tack welds. The assembled plates were then clamped against out-of-plane deformations before

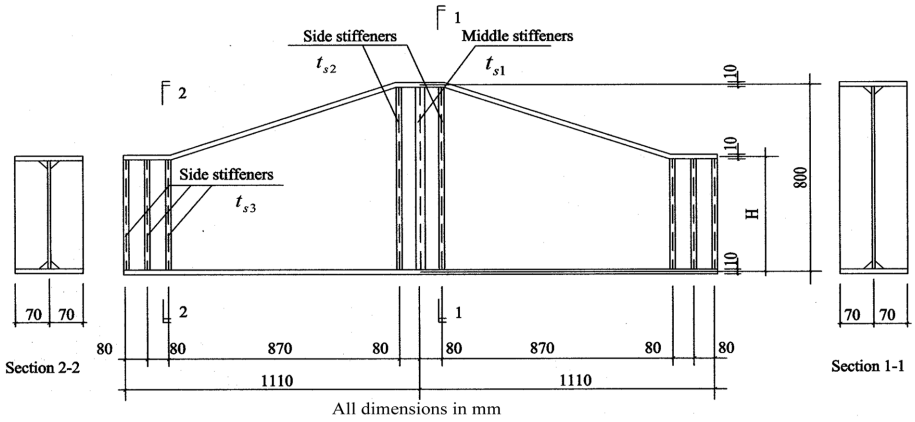

Fig. 1 Dimensions of a typical test specimen

Table 1 Measured dimensions of the test specimens

Specimen	H (mm)	t_w (mm)	t_{s1} (mm)	t_{s2} (mm)	t_{s3} (mm)
200-0	800	2.12	16.24	10.12	10.25
200-10-A	649	2.11	15.86	10.24	10.47
200-10-B	658	1.98	16.14	9.48	10.15
200-20-A	496	2.11	16.26	9.38	9.86
200-20-B	480	1.94	15.84	9.89	10.21
200-30-A	305	1.96	16.47	9.83	9.86
200-30-B	296	2.02	15.74	9.89	9.56
300-20-A	486	3.08	26.32	20.58	12.35
300-20-B	491	3.17	26.84	20.32	12.85
400-20-A	483	4.19	25.78	19.58	11.48
400-20-B	480	3.95	26.04	19.72	11.54

providing intermittent welds. Sufficient time was allowed for cooling before final continuous fillet welds were applied. Welding was carried out at different or alternate locations and the specimens were allowed to cool to minimize the effect of initial distortion caused by excessive heating at particular locations. The test specimens are identified in the text as, for example, 200-30-A, the first field viz. 200 referring to the web thickness of 2 mm, the second field 30 referring to the taper angle equal to 30 degrees and the last field A or B referring to the horizontal flange in tension or in compression in the test. All girders having label 'A' were tested with the horizontal flange in tension and those having label 'B' with the horizontal flange in compression.

2.2 Material properties

The steel plates used had a nominal yield stress equal to 280 MPa. Three coupons from each of the stock plates were tested. The stock plates refer to all plates of different thickness and from different batches. The coupon tests were carried out under displacement control in an Instron TT-KM (250 kN capacity) universal testing machine with a crosshead speed of 0.2 mm per minute. The stress-strain curves obtained in the tension tests included a linear elastic part, a distinct yield point and plateau, and an extensive strain-hardening part before necking and subsequent fracture. During all tests, the applied end displacement was paused for 1 minute to obtain the static tensile yield strength (σ_{yt}) and the static tensile ultimate strength (σ_{ut}). The average material properties such as yield stress, ultimate stress, modulus of elasticity and Poisson's ratio for series A & B are respectively 290 N/mm^2, 323 N/mm^2, 215 kN/mm^2 and 0.29 for the web-plate and flange-plates, and the corresponding values for the stiffeners were 280 N/mm^2, 304 N/mm^2, 205 kN/mm^2 and 0.27, respectively.

2.3 Test setup

A test rig built on a strong floor and capable of applying up to a maximum load of 1,000 kN was used to test the specimens. The test rig was designed to support test specimens by means of a horizontal rectangular frame. Under maximum loading, the deflection of the support frame is negligible so as to provide a perfect, non-deflecting surface. The support frame rests on the main lateral loading frame by means of a cradle. The vertical loading was applied by means of an Instron actuator capable of applying a maximum load of 1,000 kN. The point load was transferred to the specimen via a ball and socket bearing so that differential movement at failure can be prevented. The rollers sandwiched between two hardened steel raceways were inserted between the ends of the specimen and the rig to ensure a simply supported condition. A typical testing arrangement with a specimen mounted onto the rig is shown in Fig. 2. When the applied load reached a high value, it is possible for the beam to deflect in the lateral direction. The beam would, therefore, fail by lateral buckling before reaching the ultimate load. In order to prevent the beam from such a failure, it was restrained laterally by means of two tie rods: one end of the tie rod was connected to the stiffeners at the mid-span of the girder and the other end to a vertical steel member. One such typical bracing arrangement is shown in Fig. 3.

2.4 Instrumentation

The tapered plate girder was instrumented to measure vertical deflections along the span length and strain at selected locations in the web. The load-displacement plot displayed by the computer enabled monitoring of the material yielding and the onset of failure of the specimen. Readings from the strain

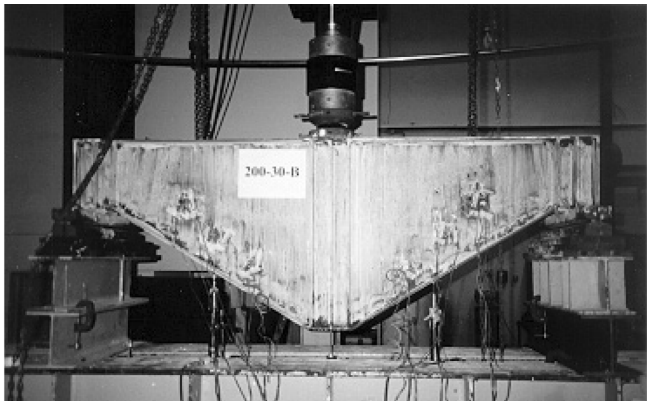

Fig. 2 A typical testing arrangement

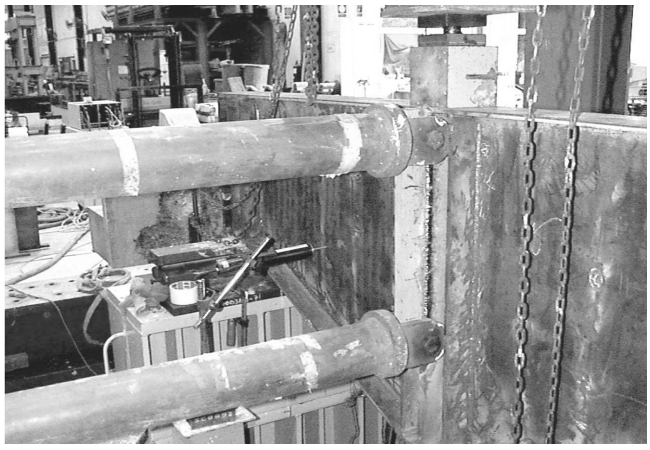

Fig. 3 A typical lateral bracing arrangement

gauges were recorded on floppy diskette using a data-logger (TD-301) connected to a computer.

2.4.1 Deflection measurement

The vertical mid-span deflections of the girder were measured by linear variable displacement transducers (LVDT) with a measurement range of 50 to 200 mm. Transducers were placed at mid-span, support and quarter span along the centerline of the girder. Taking measurements at the support is to monitor the settlement of the supports so that the actual deflection of the girder could be computed. Transducers at quarter spans on either side of the mid-span were used to monitor the symmetry in the behavior of the girder. A transducer (LVDT) was mounted onto specimens 200-20-A and 200-20-B to measure lateral deflection corresponding to the center point of the diagonal line of web-plate. Horizontal deflections were also measured at the corner of the web plate in the case of the girders 400-20-A and 400-20-B.

2.4.2 Strain measurements

Strains along the flange plate were measured by FLA-10-11 type electrical resistance strain gauges and post-yield rosettes were employed to monitor the strains on web plates. 3 rosettes were located at the center along the diagonal line at a spacing of 200 mm. Two rosettes were positioned by offsetting

the diagonal line by 200 mm on both sides. Thus, in the front surface, 5 strain rosettes were fixed and, in the back surface at the same location as those on the front side 5 rosettes were mounted. Thus, the stress distribution along the web would be monitored. Also, 3 strain gauges were placed longitudinally in the compression flange along the width, and another 3 strain gauges in the tension flange. From these strain values, the axial tension or compression force developed in flanges could be computed. For normal measurement, only 3 strain rosettes were arranged vertically across the diagonal line of the web panel with spacing of 200 mm. A typical arrangement of strain gauges is shown in Fig. 4.

2.5 Test procedure

The test procedure adopted for all specimens was the same. The specimen was mounted on the test rig with the mid-point of the girder located centrally under the jack, carefully checking by plumb. Care was taken to ensure that the specimen sits on the roller bearing and its centroidal line coincided with the centerline of the actuator applying the load. All electrical strain gauges and transducers were connected to a data acquisition system LTDS-301 programmed to record the output on a floppy diskette with simultaneous print out of the data at every load increment of 5 kN. Load-displacement and load-strain curves were plotted through a computer and it was thus possible to identify the onset of failure in the specimen. Before the actual test, a small preload of 50 kN was applied slowly on the specimen and then removed. This operation was repeated twice in order to remove any settlement in the support system and to ensure that the specimen was properly seated on the supports. At the same time, the readings of strain gauges and transducers were checked to ascertain that they functioned properly.

After ensuring that all the instruments were working satisfactorily, the strain gauges and transducers were initialized. The load was then applied on the specimen in a predetermined increment at a constant rate. After every 50 kN, the load was kept constant to allow the specimen to stabilize. At every 5 kN load increment, the strain gauges and transducer readings were recorded; the plate girder was examined for yielding. Close observations were made to locate the severe deformation of flange to form a hinge. Testing was terminated when the load dropped to one-third of the ultimate load. The ultimate load and mode of failure were recorded for each specimen.

3. Finite element modelling

The finite element program ABAQUS version 5.4 (1994), was employed to simulate the behaviour of

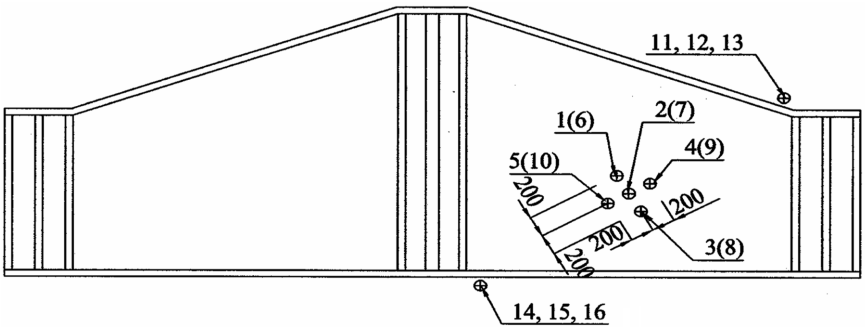

Fig. 4 Arrangement of strain gauges in a typical test specimen

the tapered plate girders. Geometric non-linear problems require kinematic relations between strains and displacements that contain second-order terms. The analysis includes both material and geometric non-linearities. The plasticity model consists of von-Mises yield surface combined with Prandtl-Reuss flow rule. The standard Newton method is used for solving the non-linear equilibrium equations. Riks Arc length method of control is used in the analyses. This method is useful in solving unstable static equilibrium problems, where the unloading path needs to be monitored. For all the analyses described, an automatic time step size was used. The post-processing stage allows the results data to be represented as deformed shapes, stress contours, colour-coded elements and yielded zones etc.

ABAQUS includes general-purpose shell elements as well as elements that are valid for thick and thin shell problems. The general-purpose shell elements provide robust and accurate solutions to most applications. However, in certain cases, for specific applications, enhanced performance may be obtained with the thin and thick shell elements; for example, if only small strains occur and five degrees of freedom per node are desired. Thin shells are needed in cases where transverse shear flexibility is negligible and the Kirchhoff constraint must be satisfied accurately (i.e. the shell normal remains orthogonal to the shell reference surface). For homogeneous shells this occurs when the thickness is less than a bout 1/15 of a characteristic length on the surface of the shells, such as the distance between supports and the wavelength of a significant eigenmode.

Since out-of plane buckling deformations are not present in perfectly flat plates under in-plane loading conditions, a small variation of $d/1000$ from flatness is introduced in order to initiate out-of plane deformations. The shapes of initial deformations were based on the buckling mode shapes. The geometry of the test specimens, loading and boundary conditions are symmetrical about the vertical line through the mid-span. The analyses were, therefore, carried out on one half of the girder and appropriate boundary conditions were used at the section of symmetry.

The numerical investigation involved three stages of analysis i.e. modelling or pre-processing, processing and post-processing. In the modelling stage, plates were first discretized into small elements using the PATRAN 7.0 package. The data from PATRAN was then converted into input data suitable for ABAQUS 5.4. The processing or analysis stage involved generation of numerical equations that describe the behaviour of the structure under a given set of boundary and loading conditions and solution of the equations as well. ABAQUS read all the relevant data defined by the input file and then carried out the numerical operation. The post-processing stage gave graphical interpretation for results generated by the processor. Typically, the deformed configuration, mode shapes and stress distributions could be computed and displayed at this stage.

A surface model consisting of 8-noded (S8R5) reduced integration quadrilateral shell elements was used to avoid any ill conditioning in the analysis. The S8R5 element that allows for changes in the thickness as well as finite membrane strains was chosen. ABAQUS package is capable of capturing the amount of initial imperfection with respect to the buckling mode displacement. A typical finite element mesh, chosen based on a series of convergence studies carried out, is shown in Fig. 5.

After the mesh generation, all mesh data are converted to standard ABAQUS input file for analysis and the elastic buckling analysis is done first. Then, the incremental-iterative load steps and required output commands need to be added in accordance with ABAQUS/Standard language. Also, the initial imperfection command, which instructs the solver to retrieve the buckling mode shape profile, needs to be included. The solution will then retrieve the contour (in terms of percentage) of specified mode shape profile as the initial geometry of the model and solve the problem from this stage. In the result file, information such as reaction, buckling or ultimate displacements can be extracted for evaluation of the buckling or ultimate load. The non-linear and large deflection analyses are used to compute the ultimate

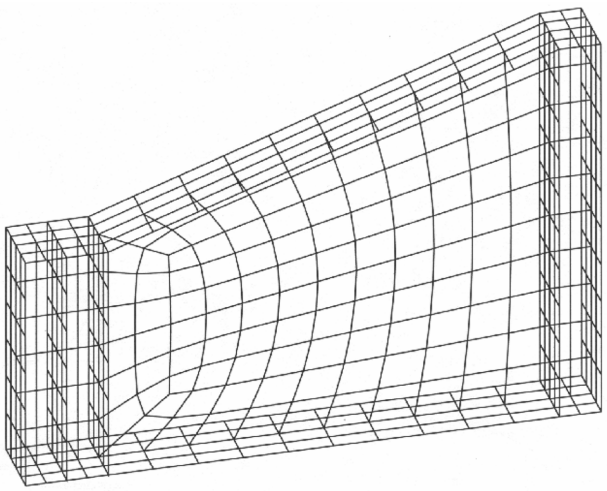

Fig. 5 A typical finite element mesh for one-half of a girder

load of the plate girder.

ABAQUS post provides graphical displays of the models and the corresponding results. Stress distribution can be presented as graphs or contour plots at any selected load and deflected shapes. A typical first buckling mode profile used as initial imperfections and stress distributions at collapse are shown in Figs. 6 and 7 respectively.

4. Experimental and finite element results

Results obtained from the experimental investigation and the finite element analyses are presented in

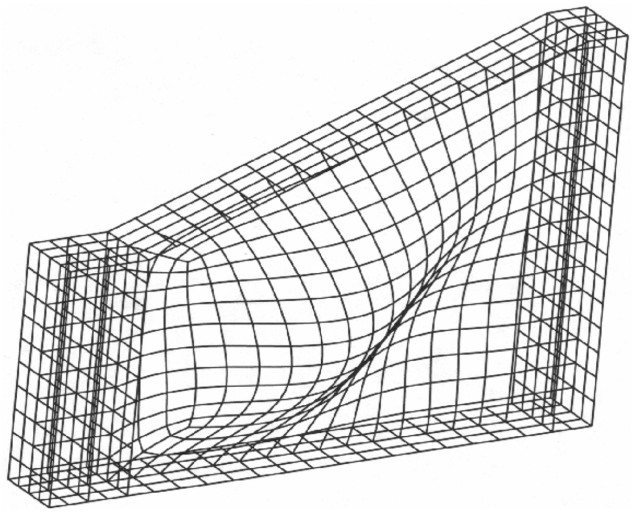

Fig. 6 Typical first eigenmode profile

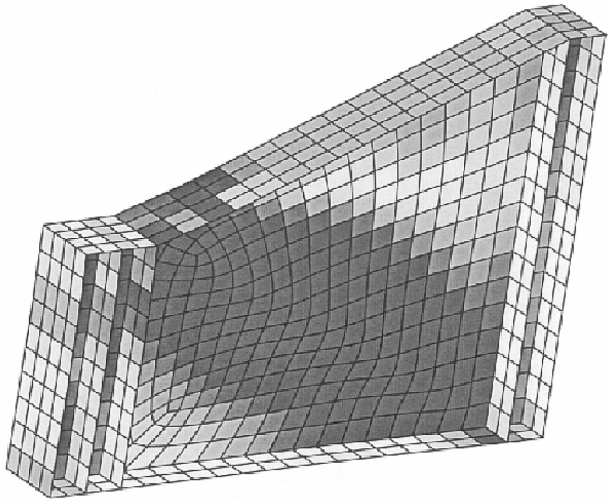

Fig. 7 A typical von-Mises stress distribution

the form of tables and figures. The load-deflection plots in the figures show the behavior from elastic to ultimate load of the girders tested. Stress distribution in webs and flanges at certain levels of load are given to show how the yielding zone develops with the increase in load. Experimental load-deflection curves are compared with those obtained from the finite element analysis to verify the accuracy of the finite element model.

Eleven specimens were tested. One of the specimens was of uniform-section and the other ten tapered girders with different combinations of taper angle, web thickness and loading direction. Experimental ultimate loads along with the corresponding values obtained from finite element analyses are summarized in Table 2 for all the tested specimens. In the table P_{FEM} refers to the finite element results, P_{TH} to the analytical results presented at the later part of the paper and P_{Test} to the experimental results. The load-vertical displacement curves obtained from the tests are plotted against the applied load in Figs. 8 and 9 for series A and B, respectively. Fig. 10 shows the load-deflection plots in which the

Table 2 Ultimate loads obtained from experiments and analytical methods numerical solution

Series	Girder No.	Theoretical solution P_{TH}, kN	Numerical solution P_{FEM}, kN	Test result P_{Test}, kN	$\frac{P_{FEM}}{P_{Test}}$	$\frac{P_{TH}}{P_{Test}}$
	200-00	320	335	327	1.02	0.98
A	200-10-A	385	337	350	0.96	1.1
	200-20-A	314	373	355	1.05	0.88
	200-30-A	377	377	359	1.05	1.05
	300-20-A	532	463	450	1.03	1.18
	400-20-A	626	596	574	1.04	1.09
B	200-10-B	304	349	320	1.09	0.95
	200-20-B	310	338	322	1.05	0.96
	200-30-B	307	314	325	0.97	0.94
	300-20-B	414	411	400	1.03	1.04
	400-20-B	528	595	578	1.03	0.91

results obtained from the experiments and finite element analyses are presented for typical girders. It can be seen from Table 2 and Fig. 10 that there is reasonable agreement between the two sets of results and the agreement is close at the initial stages of loading. The finite element results overestimate the ultimate loads for all specimens except for specimens 200-10-A and 300-20-A. The average ratio of FEM loads to experimental failure loads for the specimens tested is 1.03. This shows that the finite element modeling is capable of predicting the ultimate load-carrying capacity of tapered plate girders with reasonable accuracy in all cases.

4.1 Behavior of tapered plate girder

The load-deflection behavior and failure modes have been observed to be similar for all the specimens. It can be seen from the load - displacement plots that the curves remained linear at the initial stages of

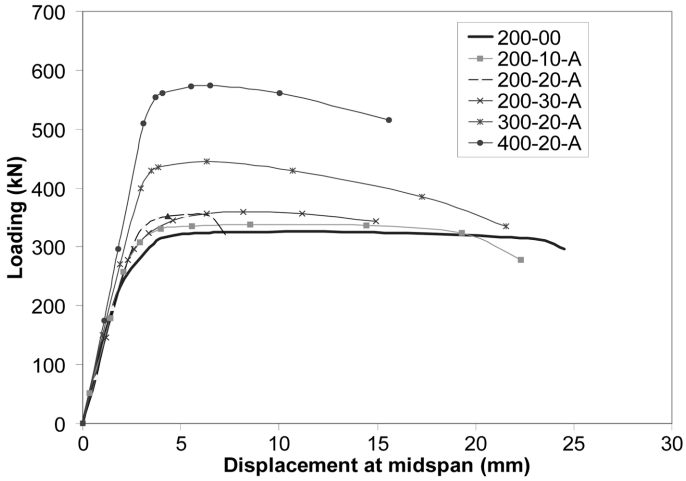

Fig. 8 Load-deflection plots for specimens tested in A series

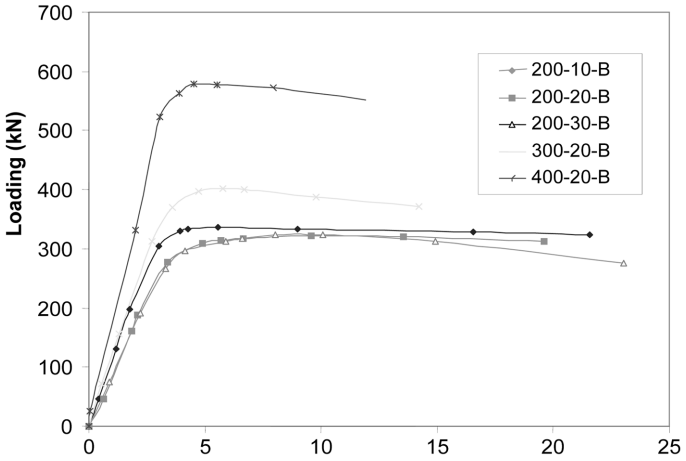

Fig. 9 Load-deflection plots for specimens tested in series B

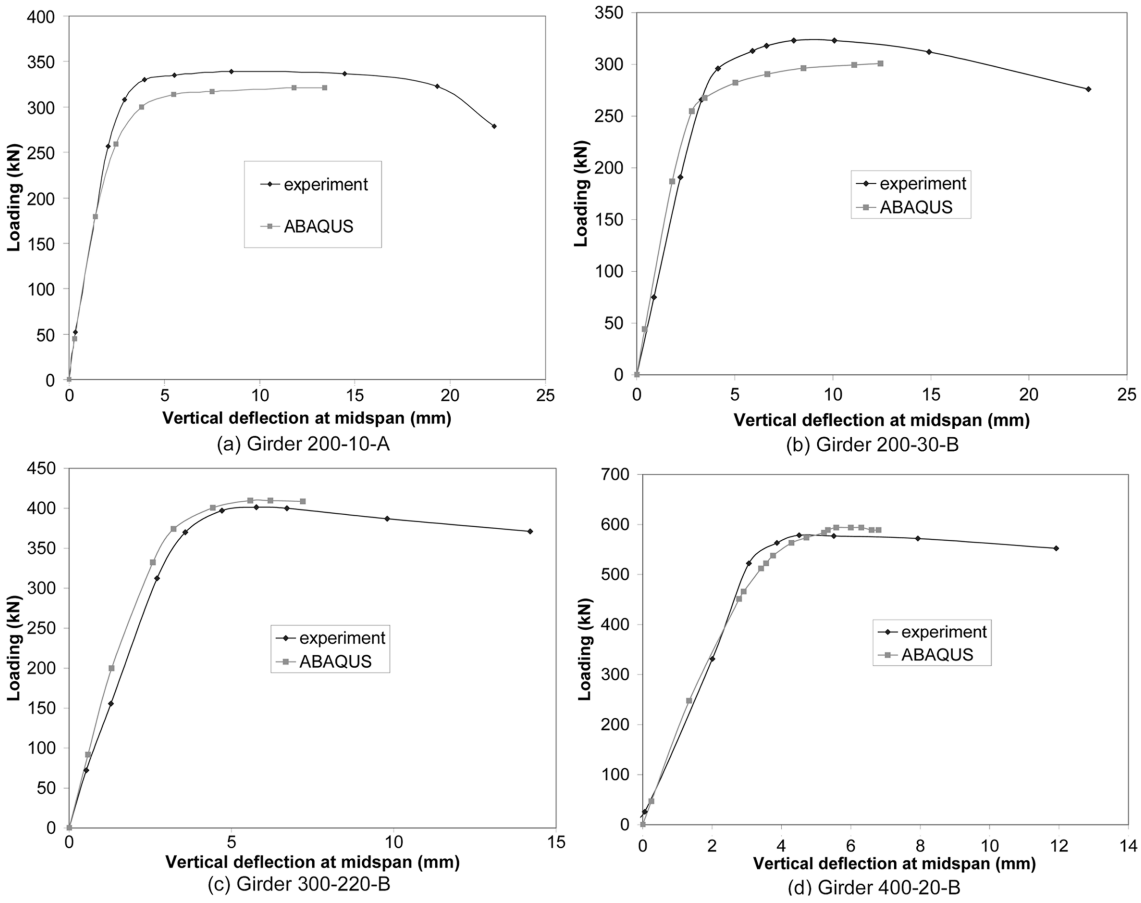

Fig. 10 Finite element and experimental load-deflection plots for typical girders

loading. When the load approached approximately one-third of the ultimate load, the web started to wrinkle slowly, and the load-deflection curve began to deviate from linear behavior. Any further increase in load did not cause a rapid collapse of the girder but resulted in the formation of buckles in a waveform parallel to the direction of the tension field. After the onset of buckling in the web, a further increase in load led to the waveform spreading along the web, and caused severe bending of the flanges due to inward pulling at four positions, two of these were located on the upper flanges, the rest on the lower flanges. When the load reached the ultimate value, the web was found to wrinkle extensively with the flange bending towards the web. Eventually, plastic hinges were formed in the flanges and the girder collapsed. As the load increased beyond the bifurcation point of the web plate, the diagonal tension developed along with the bending stresses resulting from out-of-plane deformations. With further increments of loading, material yielding began along the main diagonal tension line under the coupling action of the diagonal tension and bending, and four hinges on the upper and lower flanges formed. Depending upon the geometry, the web plate is capable of carrying additional loads in excess of that at which the web starts to buckle, due to the post-buckling reserve strength. While the load was increased, the yielding zone of the web-plate was observed to form along a diagonal band to serve as a chord, and the diagonal band kept spreading along the web with further load increase. The bending stress together

with membrane stress acts on the web, causing the material on the front and back surfaces along the diagonal line to yield consecutively.

Views after failure of typical girders are shown along with the corresponding finite element predictions in Figs. 11 to 14. Generally good agreement is observed between the deflected web profiles observed in the experiment and those obtained from the finite element analyses. Similar observations could also be made in respect of deformations in flanges.

The yield stress F_y determined for uniaxial tension is usually accepted as being valid for uniaxial compression. However, the general state of stress at a point in a thin-walled member is one of biaxial tension and/or compression, and yielding under these conditions is not so simply determined. Perhaps the most generally accepted theory of two-dimensional yielding under biaxial stresses acting in the plane is the maximum distortion-energy theory and the stresses at yield according to this theory satisfy the condition

$$f_1^2 - f_1 f_2 + f_2^2 + 3f_{12}^2 = F_Y^2$$

in which f_1, f_2 are the normal stresses and f_{12} is the shear stress at the point. In ABAQUS, the von-Mises contour feature is provided to trace how yielding area develops in the web-plate at some loading stages. Fig 15 shows the von-Mises stress distribution at specified loads at the mid-plane of the web of a typical girder. They reveal that material along its diagonal line start to yield first. With increase in load,

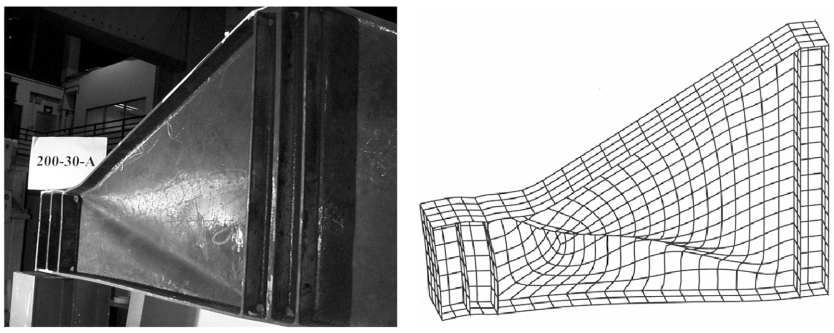

(a) Experiment (b) Finite Element Model

Fig. 11 View after failure of the girder 200-30-A

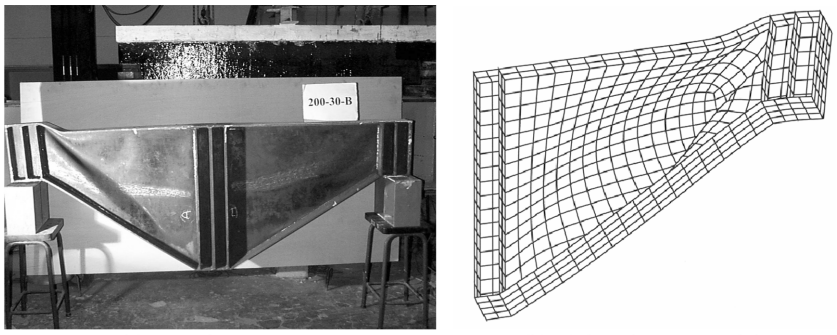

(a) Experiment (b) Finite Element Model

Fig. 12 View after failure of the girder 200-30-B

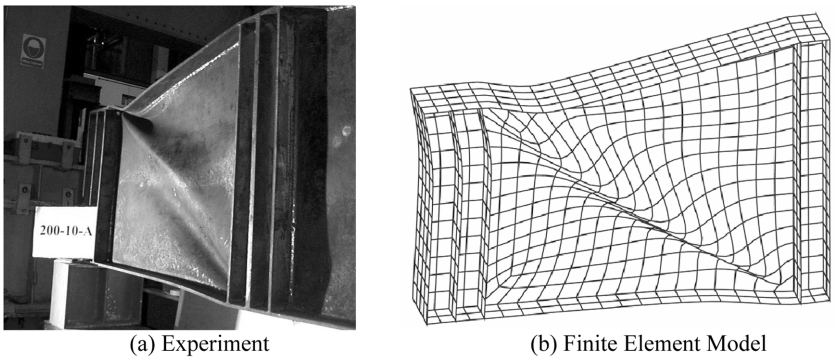

(a) Experiment (b) Finite Element Model

Fig. 13 View after failure of the girder 200-10-A

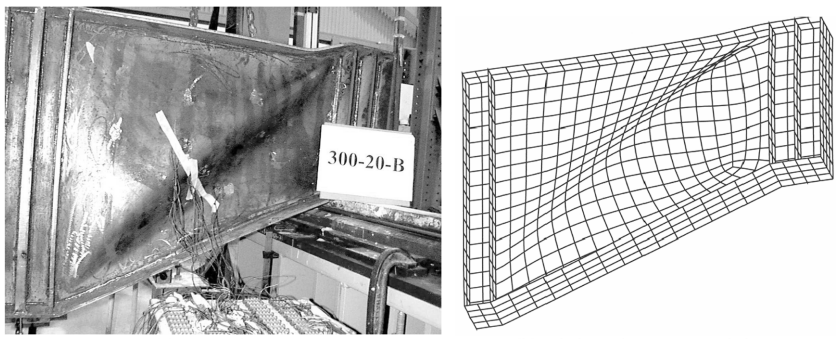

(a) Experiment (b) Finite Element Model

Fig. 14 View after failure of the girder 300-20-B

the yield zone spreads widely. The tension zone pulls up the lower flange and pushes down the upper flange to form a mechanism.

5. Analytical method

Shear in a plate girder is resisted by the web plate up to the elastic load (Fig. 16(a)). Further increase in load does not cause rapid collapse of the girder but results in the formation of buckles in a waveform parallel to the tensile direction (Fig. 16(b)). Small band of web plate along the tensile diagonal commences to behave in a manner similar to a tension member of a N-type truss. Development of membrane tension in the web is denoted as tension field action and enables the web to sustain loads well in excess of the elastic critical load. A consequence of the membrane tension in the web is the inward pulling of the flanges, under increasing loads. Eventually plastic hinges are formed in the flanges leading to collapse of the girder (Fig 16 (c)). Collapse load of a plate girder could, therefore, be assumed to consist of three components viz. (i) elastic critical load (ii) load resisted by tension field action and (iii) load contribution by the flanges. Based on this assumption Porter *et al.* (1975, 1978) proposed an equilibrium solution to evaluate the ultimate shear capacity (V_s) of a plate girder of uniform cross-section with slender webs, given by

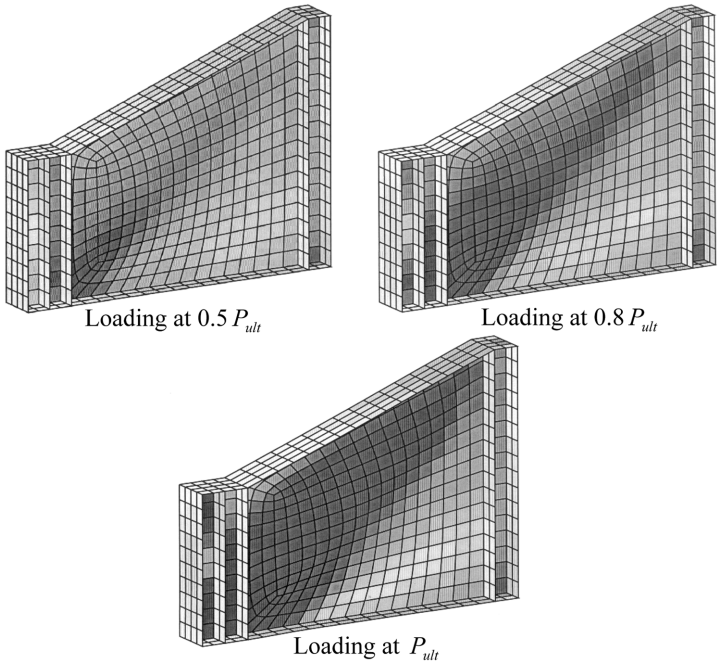

Fig. 15 von-Mises stress distribution at selected loading for typical girder

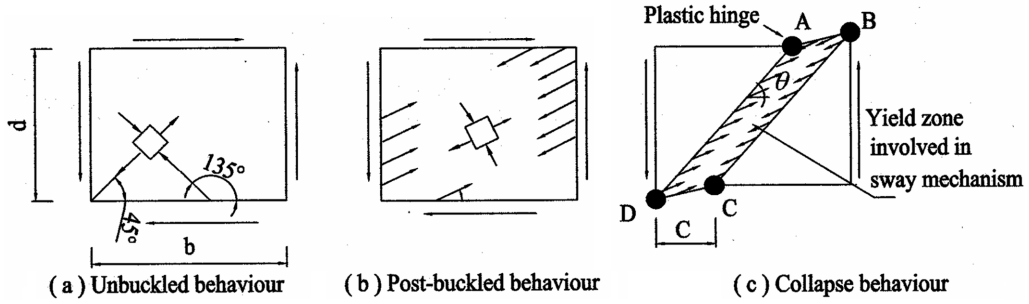

Fig. 16 Theree stages in Cardiff model (Portel *et al.* 1975)

$$V_s = \tau_{cr} dt + \sigma_t^y (d\cot\theta - b + c)\sin^2\theta + \frac{4M_{pf}}{c} \tag{1}$$

in which τ_{cr} = elastic critical shear stress for the web, σ_t^y = membrane stress in the web in the post-critical stage, b = web panel width, c = distance between the hinges formed in the flange, d = web depth, t = web thickness, θ = angle of inclination of the tensile membrane stress σ_t^y and M_{pf} = plastic moment of the flange.

'c' is obtained from

$$c = \frac{2}{\sin\theta}\sqrt{\left(\frac{M_{pf}}{\sigma_t^y t}\right)} \tag{2}$$

Membrane stress σ_t^y is obtained as

$$\sigma_t^y = -\frac{3}{2}\tau_{cr}\sin 2\theta + \sqrt{\left(\sigma_{yw}^2 + \tau_{cr}^2\left\{\left(\frac{3}{2}\sin 2\theta\right)^2 - 3\right\}\right)} \tag{3}$$

The elastic critical stress in shear τ_{cr}, for the web is given as

$$\tau_{cr} = k\frac{\pi^2 E}{12(1-\nu^2)}\left(\frac{t}{d}\right)^2 \tag{4}$$

Where k for a web fixed along the edges is given by

$$k = 8.98 + 5.6\left(\frac{d}{b}\right)^2 \qquad \text{for}\left(\frac{b}{d} > 1.0\right) \tag{5}$$

Finally, θ in the failure mechanism is evluated to obtain a maximum value for V_s.

In the case of a tapered plate girder supported at its ends and subjected to a concentrated load applied at the mid-span two cases viz. (i) with inclined flange under tension and (ii) with inclined flange under compression, as shown in Fig 17, is considered. Elastic buckling equation is assumed to correspond to that of plate girders of uniform cross-section along the span with web depth 'd' of a panel taken as the average value of the depths at the support and at the mid-span. Therefore, in Eq. (4), d is $d' = 1/2(d_1 + d_2)$, where d_1 and d_2 are web depths at the support and at the line of symmetry, respectively.

For a plate girder with inclined flange in tension, once the web has yielded, final failure of the girder will occur when plastic hinges have formed in the flanges, as shown in Fig. 18 (a). It is a minimum requirement that the region *ABCD* of the web yields before a mechanism can develop, although the yield zone may well spread outside this region. The failure load may be determined by applying a virtual sway displacement to the girder in its collapse state.

It is convenient to consider the yielded region *ABCD* of the web panel to be removed and to replace its action upon adjacent flange and web regions by the tensile membrane stresses, as shown in Fig 18(b). Those stresses acting on the stationary section *AD* obviously do no work during the virtual displacement. Thus, the only membrane stresses that will do any work are those acting on the faces *AB*, *BC* and *CD*. With due consideration to the fact that c_c and c_t are not equal, c_c is approximately taken equal to c given by Eq. (2) and the length c_t given by

$$c_t = \frac{2}{\sin|\varphi - \theta|}\sqrt{\left(\frac{M_{pf}}{\sigma_t^y t}\right)} \tag{6}$$

in which σ_t^y = membrane stress to produce yield, t = thickness of web, θ = inclination of membrane

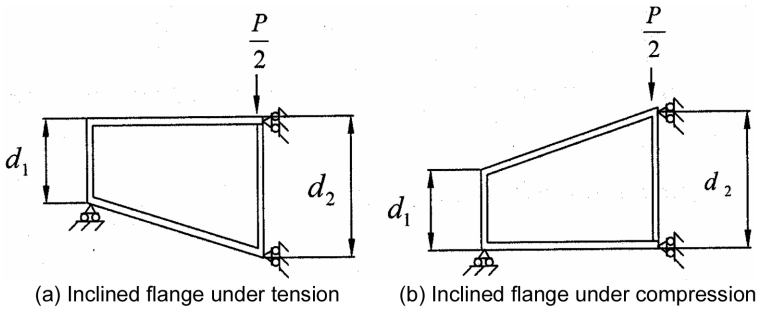

(a) Inclined flange under tension (b) Inclined flange under compression

Fig. 17 Tapered plate girder

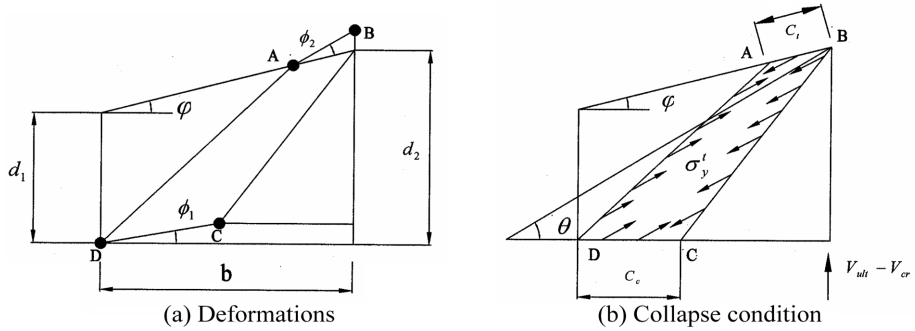

(a) Deformations (b) Collapse condition

Fig. 18 Case of inclined flange under tension

stress, φ = taper angle, c_t = length of plastic hinge in tension flange and

$$2M_{pf} = \sigma_y^t t \frac{c_t^2}{2} \sin(\theta - \varphi)$$

Ultimate shear capacity V_{ult} can be obtained as

$$V_{ult} = V_{cr} + \frac{\sigma_y^t t c_t \sin(\theta - \varphi)\sin\theta}{2} - \frac{\sigma_y^t t c_c \sin^2\theta}{2} + \sigma_y^t t(d\cot\theta - b + c_c)\sin^2\theta + 2M_{pf}\left(\frac{1}{c_c} + \frac{1}{c_t \cos\varphi}\right) \quad (7)$$

For a given size of plate girder, the only unknown in Eq. (7) is θ. The maximum value of V_{ult} can be obtained by trial and error to yield an optimum value for θ.

In a similar manner, V_{ult} for the case of a girder with inclined flange under compression can be determined by considering the mechanism as shown in Fig. 19 as

$$V_{ult} = \frac{1}{1 - \frac{tb}{2d}\tan\varphi}(A + B - C) + 2M_{pf}\left(\frac{1}{c_t} + \frac{1}{c_c \cos\varphi}\right) + V_{cr} \quad (8)$$

Where $A = \sigma_y^t t[(d'\cot\theta - b)\sin\theta + c_c \sin(\varphi + \theta)]\sin\theta$

$$B = \frac{\sigma_y^t t c_c \sin^2\theta}{2}$$

$$C = \frac{\sigma_y^t t c_c \sin^2(\theta + \varphi)\sin\theta}{2}$$

$$2M_{pf} = \sigma_y^t t \frac{c_c^2}{2} \sin^2(\theta + \varphi)$$

All the test girders were analysed using Eqs. (7) and (8) and the ultimate loads thus obtained are listed in Table 2. The agreement between the predicted values and the corresponding test results is reasonably good, except in the case of girders 200-20-A and 300-20-A. Considering the approximations used in the analysis it can be concluded that the analytical method is capable of predicting the ultimate failure load

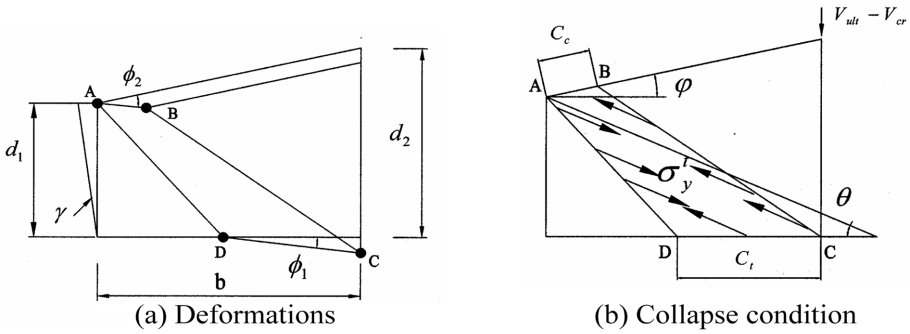

Fig. 19 Girder with inclined flange under compression

of tapered plate girders accurately.

6. Conclusions

Both experimental and theoretical methods of study on the behaviour and load carrying capacity of tapered plate girders have been described in this paper. Based on the results presented herein it can be concluded that the proposed three dimensional finite element modelling using the software package ABAQUS is reliable in predicting the ultimate shear strength of the tapered plate girders with sufficient accuracy. If inclined flanges are under tension, the taper angle in the range studied herein has a moderate influence over shear capacity of the tapered girder. Compared to the shear capacity of a girder of uniform section, a 5 % loss in shear strength may occur. Whilst inclined flanges are subjected to compression, the ultimate load of tapered girder becomes higher than that of the straight girder by more than 5%. A more comprehensive study is needed to evaluate the effect of parameters such as taper angle, web slenderness, flange stiffness and web panel aspect ratio on the behaviour and ultimate load of the tapered girders. The proposed analytical method is found to predict the ultimate load with sufficient accuracy.

Acknowledgements

The investigation described in this paper has been carried out at the Department of Civil Engineering, National University of Singapore. The support by Yongnam (Singapore) Pte Ltd who supplied the test specimens is greatly appreciated.

References

ABAQUS Theory Manual Version 5.4, Hibbit, Karlsson & Sorensen, Inc., USA., 1994.
ABAQUS User's Manual Version 5.4, Hibbit, Karlsson & Sorensen, Inc., USA., 1994.
ABAQUS/POST Manual Version 5.4, Hibbit, Karlsson & Sorensen, Inc., USA., 1994.
Baskar, K., Shanmugam, N. E. and Thevendran, V. (2002), "Finite element analysis of steel-concrete composite plate girders", *J. Struct. Eng., ASCE*, USA, **128**, (9), 1158 -1168.
Baskar, K. and Shanmugam, N. E. (2003), "Steel-concrete composite plate girders subject to combined shear and bending", *J. Constr. Steel Res.*, UK. **59**(4), 531-557.

Calladine, C. R. (1973), "Plastic theory for collapse of plate girders under combined shearing force and bending moment", *Structural Engineer*, **51**(4), 147-154.
Davis, G and Mandal, S. N. (1979), "The collapse behaviour of tapered plate girders loaded within the tip". *Proceedings of the Institution of Civil Engineers,* Part 2, **67**, pp.65-80.
Evans, H. R., Porter, D. M. and Rockey, K. C. (1978), "The collapse behavior of plate girders subjected to shear and bending", *Int. Ass. Bridge Struct. Eng, Periodical, Proc*. P-18/78.
Graciano, C. A. and Edlund, B. (2002), "Nonlinear FE analysis of longitudinally stiffened girder webs under patch loading", *J. Constr Steel Res.*, **58,** 1231-1245.
Graciano, C.cA. (2003), "ultimate resistance of longitudinally stiffened webs subjected to patch loading", *Thin-Walled Struct.*, 41, 529-541.
Jung, S. K. and White, D. W. (2006), "Shear strength of horizontally curved steel I-girders finite element analysis studies", *J. Constr. Steel Res*., **62**,329-342.
Kim, J. T., Park, J. H. and Lee, B. J. (2007), "Vibration-based damage monitoring in model plate- girder bridges under uncertain temperature conditions", *Eng. Struct.*, **29**, 1354-1365.
Lian, V. T. and Shanmugam, N. E. (2003), "Openings in horizontally curved plate girders", *Thin-Walled Struct*., UK, **41**(2-3), 245-269.
Lian, V. T. and shanmugam, N. E. (2004), "Design of horizontally curved plate girder webs containing circular openings", *Thin Walled Struct*., UK, **42**(5), 719-739.
Owen, D. R. J., Rockey, K. C. and Skaloud, M. (1970), "Ultimate load behavior of longitudinally reinforced web plate subjected to pure bending", *IABSE Publications*, 113-148.
Park, Y. H., Park, C. and Park Y. G. (2005), "The behaviour of an in-service plate girder bridge strengthened with external prestressing tendons", *Eng. Struct.*, **27**, 379-386.
Porter, D. M., Rockey, K, C, and Evans, H. R. (1975), "The collpase behaviour of plate girders loaded in shear", *Structural Engineer*, **53**, 313-325.
Roberts, T. M. and Rockey, K. C. (1979), "A mechanism solution for predicting the collapse loads of slender plate girders when subjected to in-plane patch loading", *Proceedings of the Institution of Civil Engineers,* Part 2, **67**, 155-175.
Roberts, T. M. and Markovic, N. (1983), "Stocky plate girders subjected to edge loading", *Proceedings of the Institution of Civil Engineers*, Part 2, **75**, 539-550.
Roberts, T. M. (1981), "Slender plate girders subjected to edge loading", *Proc. Inst. Civ. Engr.*, Part 2, **71**, 805-819.
Roberts, T. M., Newark, A. C. (1996), "Shear strength of tapered aluminium plate girders", *Bicentenary conference on Thin-Walled Structures*, Galsgow.
Roberts, T. M and Newark, A. C. B. (1997), "Shear strength of tapered aluminium plate girders", *Thin-Walled Struct.*, **29**(1-4), 47-58.
Roberts, T. M. and Shahabian, F. (2001), "Ultimate resistance of slender web panels to combined bending shear and patch loading", *J. Constr. Steel Res*, **57**, 779-790.
Rockey, K. C. (1968), "Factors influencing ultimate behaviour of plate of plate girders", *Conference on Steel Bridges*, June 24-30, British Constructional Steelwork Association, Institution of Civil Engineers, London.
Rockey, K. C., & Skaloud, M. (1972), "The ultimate load behaviour of plate girders loaded in shear", *The Structural Engineer*, **50**(1) 29-48.
Ryu, H. K., Chang, S. P., Kim, Y. J. and Kim, B. S. (2005), "Crack control of a steel and concrete composite plate girder with prefabricated slabs under hogging moments", *Eng. Struct*, **27**, 1613-1624.
Skaloud, M. and Rockey, K. C. (1971), "Ultimate load behaviour of plate girders loaded in shear", *IABSE Proc.,* 1-19.
Shanmugam, N. E. and Baskar, K. (2003), "Steel-concrete composite plate girders subject to shear loading", *J. Struct. Eng., ASCE.* USA, **129**(9), 1230-1242.
Shanmugam, N. E. and Baskar, K. (2006), "Design of composite plate girders under shear loading", *Steel Compos. Struct*, **6**(1), 1-14.
Shanmugam, N. E., Mahendrakumar, M. and Thevendran, V. (2003), "Ultimate load behaviour of horizontally curved plate girders", *J. Constr. Steel Res.*, UK, **49**(4), 509-529.
Sharp, M. L., and Clark, J. W. (1971), "Thin aluminum shear web", *J. Struct. Div., ASCE*, 1021-1038.